Thermal performance of self-rewetting gold nanofluids: application to two-phase heat transfer devices

Ibrahim Zaaroura, Souad Harmand, Julien Carlier, Malika Toubal, Aurélie Fasquelle, Bertrand Nongaillard

HAL Id: hal-03364917
https://hal.science/hal-03364917

Submitted on 24 Apr 2023

Thermal performance of self-rewetting gold nanofluids: Application to two-phase heat transfer devices

Ibrahim Zaaroura *[a, b], Souad Harmand*[a], Julien Carlier [b], Malika Toubal [b], Aurélie Fasquelle [c]
Bertrand Nongaillard [b]

a- Univ. Polytechnique Hauts-de-France, CNRS, UMR 8201- LAMIH - Laboratoire d'Automatique de Mécanique et d'Informatique Industrielles et Humaines, F-59313 Valenciennes, France

b- Univ. Polytechnique Hauts-de-France, CNRS, Univ. Lille, YNCREA, Centrale Lille, UMR 8520 - IEMN -DOAE, F-59313 Valenciennes, France

c- Jeumont Electric, 59460 Jeumont, France

Abstract

This paper presents an experimental analysis of the phenomenon of phase change inside a porous medium using different types of working fluids. It represents the impact of these fluids on improving the characteristics of heat and mass transfer in a Capillary Heat Pipe (CHP). In this study, gold nanoparticles (5 nm in diameter with 1% C_v), a self-rewetting binary solution (butanol with 3% C_v), and a mixture of self-rewetting butanol and gold nanofluid are considered to be the operating fluids within the CHP. The experiments are carried out after designing and developing the capillary heat pipe section. It consists of a water tank with a pump, an evaporator attached to a copper porous medium on which thermocouples and power supplies are placed. The experimental results showed the positive influence of gold nanoparticles on the thermal system's performance by reducing the thermal resistance by 13% compared to pure water as the base working fluid. In addition, a self-rewetting butanol solution showed improvement in the performance of the capillary evaporator by decreasing its casing temperature. While a mixture of self-rewetting butanol solution (3 % C_v) and gold nanofluid (1% C_v) exhibited the best performance of heat and mass transfer performance by reducing the thermal resistance of the system by approximately 22 %. To explain the mechanism for improving heat transfer, the phase change phenomenon was visualized by an infrared camera for the three working fluids. It is shown that as the applied power increases, the shape of the vapor pocket developed in the wick also increases, for pure water, until it reaches a stable form. Whereas, with respect to nanofluid and self-rewetting fluid, the shape of the vapor pockets was smaller than that of pure water allowing more efficient mass and heat transfer. The thermophysical properties of these fluids such as thermal conductivity, stability, surface tension, Marangoni, wettability, and capillary forces were presented to ensure and validate the decrease in the vapor pocket as well as the enhancement of the CHP thermal system.

Keywords: Gold nanofluids; Self-rewetting fluids; Heat pipes; Phase change; Visualization.

List of Symbols

CHP	Capillary Heat Pipe
% C_v	Volume Concentration, %
LHP	Loop Heat Pipe
CuO	Copper oxide nanoparticles
Au	Gold nanoparticles
Bu	Butanol solution
σ	Surface tension, N/m^2
r_p	Pore radius, m
θ	Contact angle, °
Δh	Hydrostatic pressure, m
$\emptyset$	Applied power, W
V	Voltage, U
I	Current, A
T_c	Casing temperature, °C

$T_{w,in}$ Inlet wick temperature, °C

R_T Thermal resistance, °C/W

1. Introduction

Heat removal is an important parameter while designing compact electronic components. Initially copper heat sinks were used to remove the heat from electronic mother board. Nowadays, to increase the heat transfer in these systems, like laptops, note book computers etc., heat pipes have been used. The evolution of the electronic and electrical industries requires thermal control and improvement techniques to ensure its functionality and reliability [1-3]. Thus, as a fundamental discipline of thermal engineering with many applications, heat transfer is becoming an important topic which attracts researchers looking for recovery methods [4-6]. One of the improvement methods is the modern nanotechnology known as nanofluids [7-10]. Nanofluids are suspensions of nano-size particles (from 2 to 100nm) in liquids with different types of nanoparticles such as copper oxide, aluminum oxide, silicon oxide and so on. Several research projects (since 1990) indicated that the addition of small amounts of nanoparticles in liquids can increase significantly the effective conductivity in the range 10-50% as well as their convective heat transfer coefficients. [11-14] For this raison, nanofluids are used in different industrial applications such as cooling of electronic components, automotive, enhanced oil recovery (EOR), nuclear and so many [15-17].

One of the most important applications under investigation nowadays is to study the properties of nanofluids for heat pipes [18-20]. The life time of an integrated circuit (IC) used in electronic devices depends on its operating temperature creating a trade-off situation either to enlarge the package to accept additional cooling or to sacrifice IC lifetime. Among other cooling techniques, heat pipes emerged as the most appropriate technology and cost effective thermal design solution due to its excellent heat transfer capability (high effective thermal conductivity), high efficiency, passive operation and structural simplicity (lower costs). The heat pipe is a vapor-liquid phase change device that transfers heat from a hot side to a colder side using capillary forces generated by a wick or porous material and a working fluid [21, 22]. They are made of a tube, in the most of the cases metal tube to achieve the highest thermal conductivity, and partially charged with an operating fluid. The main parts of the heat pipes are evaporator and condenser, see **Fig. 1**. Two different loops of heat pipes can be used for cooling electronic devices, Capillary Pumped Loop (CPL) and Loop Heat Pipe (LHP). Both devices consist of an evaporator, a condenser, a reservoir (a compensation chamber) and vapor and liquid lines (See **Fig. 1 (a)**). Thus, they use

capillary action in the evaporator section, (See **Fig. 1(b)**), to remove heat from the source and passively move it to a condenser side. These devices are using the fluid circulation and the vaporization phenomena inside the porous wick to transport large heat load without the need for a mechanical pump [23].
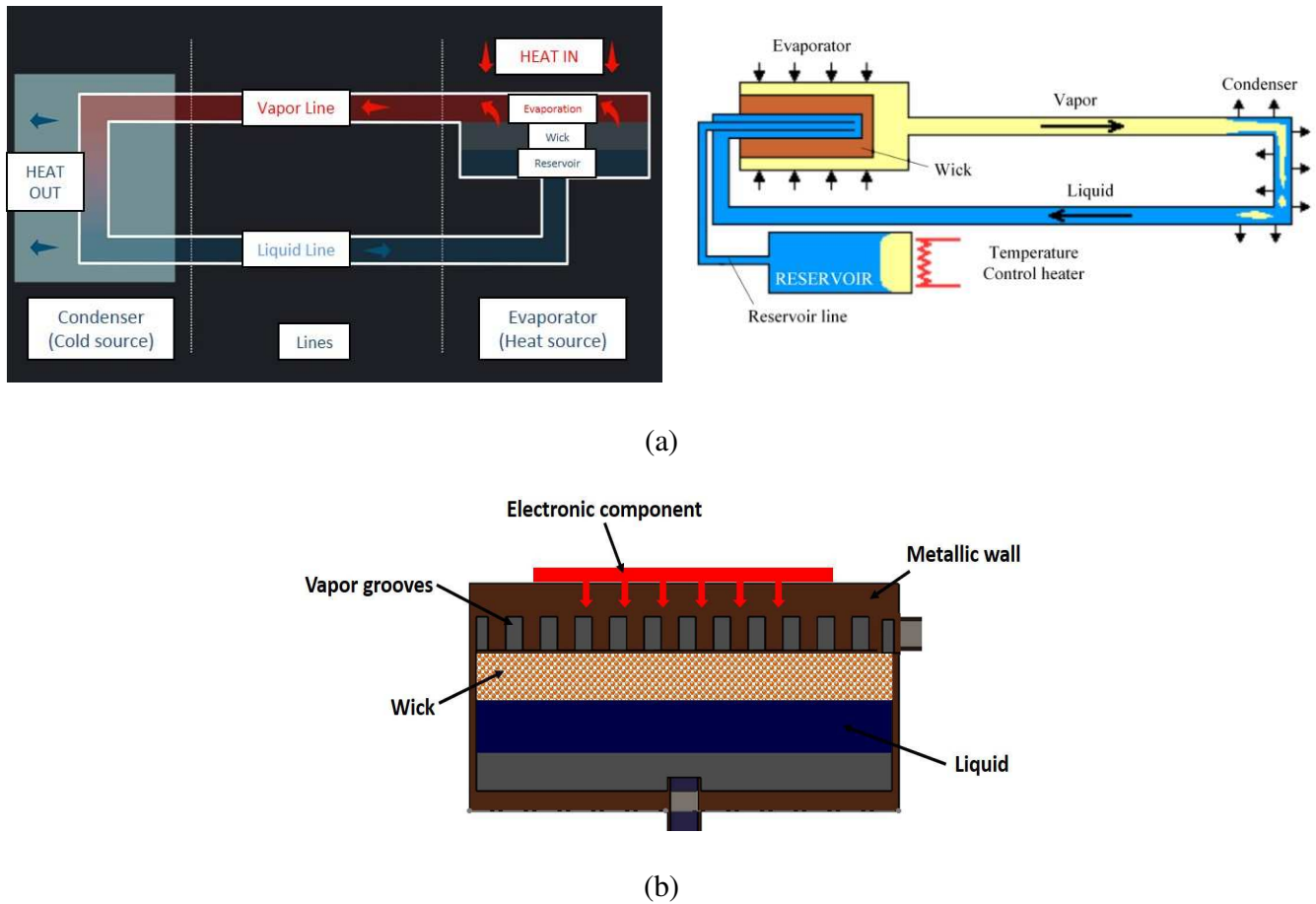

(a)

(b)

Figure 1. (a) LHP (Left side) and CPL (Right side) design, (b) Capillary evaporator. [24]

Fig. 1(b) shows the evaporator section that is responsible for the liquid circulation during a full loop operation thanks to the capillary pressure generated inside the porous medium. This section represents the most important part of the LHP and CHP.

Self-rewetting fluid is another type of fluids that has also been studied in particular for improving heat pipes. Using this type of fluids, two additional forces represented by thermal and concentration Marangoni forces can be identified in grooved pipes at the film-vapor interface.

These forces added an additional mechanism able to pump the liquid phase away from the condenser other than the gravitational and capillary ones. In the literature, many efforts have been devoted to study the influence of different types of working fluids such as nanofluids and binary mixture fluids (called as self-rewetting fluids) on heat transfer systems performance. So, these fluids were proposed for the first time by Abe and Savino [25-27]. Savino et al. [28] investigated experimentally and numerically the thermal performance of self-rewetting fluids in an innovative heat pipes. Analysis done by visualize the flow in a groove heat pipe where the Marangoni convection presented a major role on the heat transfer enhancement.

The results obtained showed that the heat pipes operating with binary mixtures fluids exhibited better thermal performance by reducing the thermal resistance by 26% for Heptanol, Hexanol and Pentanol compared to pure water. Later on, Savino et al. [29] experimentally studied the effect of Marangoni flow on the dry out limit in heat pipes systems. The advantage of using binary mixtures is that their surface tension variation has a positive slope, at a certain temperature, as a function of temperature [30]. Moreover, the addition of nanoparticles to a working fluid, pure water or binary mixtures, can increase the thermal performance of heat pipe by increasing the CHP and the overall boiling limit of heat pipes. Teng et al. [31] used an experimental analysis and found that the alumina nanofluid is one of the most efficient nanofluids for use in heat pipes. The thermal efficiency of heat pipes has been found improved by 16.8 % which is higher than that of heat pipe charged with distilled water. Also, Kang et al. [32] found success with 35 nm silver nanoparticles reducing in thermal resistance from 0.004-0.005 °C/W to 0.001-0.002 °C/W for different power loads.

In order to improve the performance of heat pipes, different analysis and limitation should be considered. At steady-state, a two-phase heat transfer system could face many limitations during heat transport such as a capillary, over heat limit and boiling. The capillary limit is reached, during the operation, when pressure losses in the entire loop exceed the maximum capillary pressure generated within the porous medium. The maximal capillary pressure is defined by the Young-Laplace's law:

$$\Delta p_{tot} \geq \Delta p_{cap,max} \qquad\qquad \Delta p_{cap,max} = \frac{2\sigma \cos\theta}{r_p}$$

Where σ denotes the surface tension, r_p denotes the pore radius and θ denotes the contact angle between the liquid and the wick. Thus, the heat transfer enhancement is due to the marangoni forces caused by temperature gradient which provide an additional mechanism for the return liquids from the condenser to the evaporator, other than capillary forces.

In this work, an experimental study is focused on the impacts of very small size of gold nanofluid (Au/water) (5 nm), a self-rewetting fluid (butanol/water) on heat and mass transfer in a two-phase capillary heat pipe. An additional novelty in this work is added to observe the impact of the combination of self-rewetting fluid (butanol) and gold nanoparticle in one single working fluid. This method can open access to analyze different physical phenomena and properties in a working fluid. As a result, a clear explanation can be introduced about the combination in gold nanoparticles' thermal conductivity enhancement as well as the thermal and concentration Marangoni forces of butanol.

The analysis is carried out on the evaporator which is the most important element of the CHP, **Fig. 1 (b).** The selected working fluids were based on their thermal performance: Marangoni lifetime, thermal conductivity, evaporation rate, capillary forces. [33, 34]

2. Experimental set-up and procedure

2.1. Working fluids:

The studied fluids in the present work consist of: gold (Au) nanoparticles (Sigma Aldrich, Molecular weight = 196.97 g/mol with a volume concentration of 1% C_v), self-rewetting fluid (butanol) and a mixed of self-rewetting butanol and gold nanofluid dissolved in distilled water (as a base fluid) and all are stabilized through ultrasonication (Elma, S 10/H) for at least 30 min before use. The size of gold nanoparticles particle was 5nm for the 0.1mM PBS, reactant free, **Table. 1**.

Fluids	Size (nm)	Concentration, Cv%	Buffer solutions
Au/water	5	1%	0.1mM PBS, reactant free
Butanol/water	-	3%	-
Au/Butanol/water	-	1%-3%	-

Table 1. Working fluids and concentrations used.

2.2. Method:

The experimental setup shown in **Fig. 2** represents a clear description of the CHP evaporator section. The system is made of a copper porous material with its properties given in **Table. 2** attached to a flat evaporator section (3.5 x 0.3 x 1.5 cm) with grooves brass block. A transparent window made of sapphire (5 x 1 cm) was used to enable the transmission and visualize the liquid/vapor phase change inside the porous wick with a high infrared camera (FLIR, SC7210-7500/SC7300, 320 x256 Pixels, and 30 μm detector pitch - **Appendix A**) during operation. Emissivity control has been taken into account for fluids and copper porous medium as well as the sapphire crystal with its characteristics related to infrared measurements. The emissivity was set to ε= 0.96 during the visualization.

The upper copper surface of the porous wick is heated with cartridge heaters at different input powers. The heating block was well insulated with multilayer insulation materials to avoid the heat losses to ambient temperatures. Throughout the experiment, the evaporator was connected to a constant level to reservoir to supply sub cooled fluid to the compensation chamber connected (5 x 1.5 x 2 cm) to the wick under the same conditions.
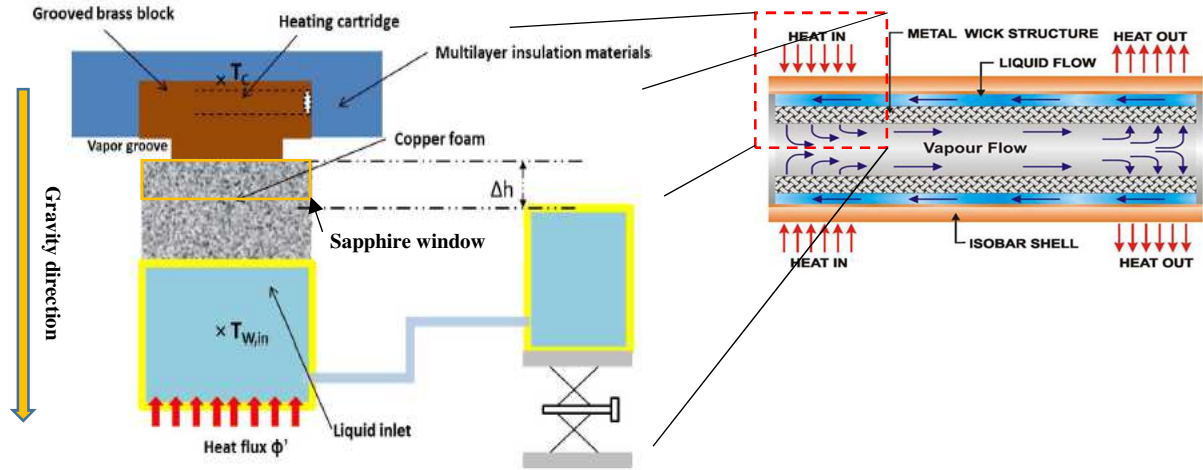

Figure 2. Experimental setup of the evaporation part.

This constant level is defined by the hydrostatic pressure drop which is controlled by Δh. The liquid inside the tank was at room temperature and a heating resistor film is used to heat the fluid

before entering the porous medium. Two K-type thermocouples are used to measure the casing temperature T_c and the temperature of the fluid at the wick inlet $T_{w, in}$. The flow rate of the fluid at inlet was same and controlled by the pump during whole experiments. Whereas, the experiment are carried out under normal pressure condition.
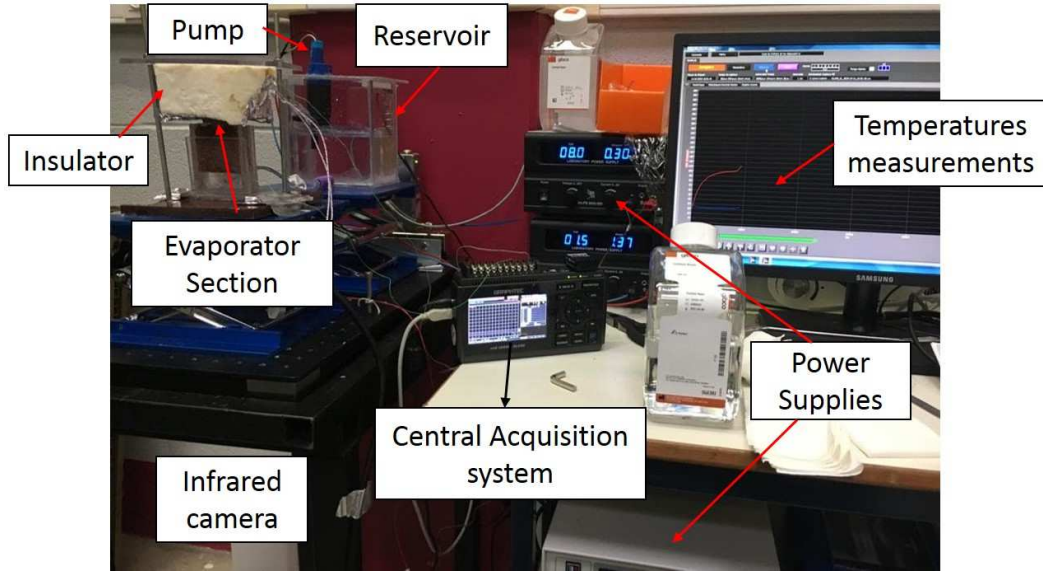

Figure 3. Experimental setup in real state.

2.3. Error Analysis:

The error analysis was taken into account for the experimental measurements. The fluid's temperatures at the wick inlet and the casing are measured by using K-type thermocouples. The measurement uncertainties are around ±1 °C. While with respect to input powers, the relative uncertainty is estimated as 3.18% and it is determined by using following equation: [35]

These error analyses were found after representing the repeatability of the measurement for each fluid used in the CHP.

$$\frac{\delta_\emptyset}{\emptyset} = \sqrt{\left(\frac{\delta V}{V}\right)^2 + \left(\frac{\delta I}{I}\right)^2}$$

Where $\emptyset$ denotes the applied heat load, V is the voltage and I is the current.

2.4. Porous media properties and systems' thermal resistance

The real sample of copper wick structure is shown in **Fig. 3**. The dimensions of the porous wick are 5 x 1.5 x 5 cm. The properties of the wick are listed in Table. 1.
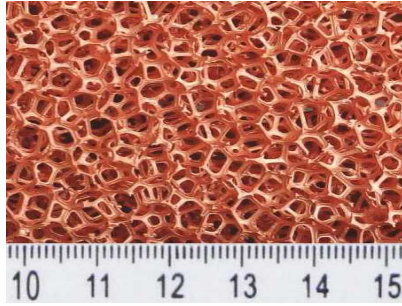

Figure 1. Wick Image

Mean Pore diameter (mm)	0.638
Porosity (%)	96
Permeability (m^2)	**1.238 10^{-6}**
Effective thermal conductivity (W/mK)	**16.24**

Table 2. Porous media properties

In order to describe the thermal performance of the evaporator, we define the evaporator thermal resistance (Coefficient of heat transfer) as follows:

$$R_T = \frac{T_c - T_{w,in}}{\varnothing}$$

Where $\varnothing$ refers to the power applied to the evaporator, T_c is the casing temperature and $T_{w,in}$ is the liquid temperature at the wick inlet.

3. Experimental Results and discussion

3.1. Heat transfer characteristics

Casing temperature, T_c, was measured and presented as a function of applied power for different fluids used in this experiment (Pure water, butanol solution and gold nanofluids). **Fig. 4**. Describes the temperature evolution of the casing temperature for different working fluids at

steady state. First experiment was done using pure water liquid as a reference to this work in order to observe the effect of other liquids on convective heat transfer coefficient, h °C/W.

This figure shows that as the heat load increases, the temperature of the evaporator also increases. These values of heat load were set after the analysis done in [36] to select the good range limit compared to heat transfer coefficient and the adverse hydrostatic head.

Both of gold nanofluid and butanol aqueous solution, the casing temperature is always lower than that pure water. During the operation of an evaporator filled with gold nanofluid (1% C_v), the casing temperature is approximately 145 °C whereas for the pure water the temperature is about 155 °C for a heat load of 85 W. While for the self-rewetting butanol solution with 3% C_v, the casing temperature was 140 °C which is less than the gold nanofluids. Finally, a mixture of self-rewetting butanol and gold nanofluid with 1% Au and 3% butanol exhibits the best performance with 137 °C for the same heat load 85 W. The over heat in the evaporator casing was higher for water because the vapor pocket developed inside the porous wick was large too.
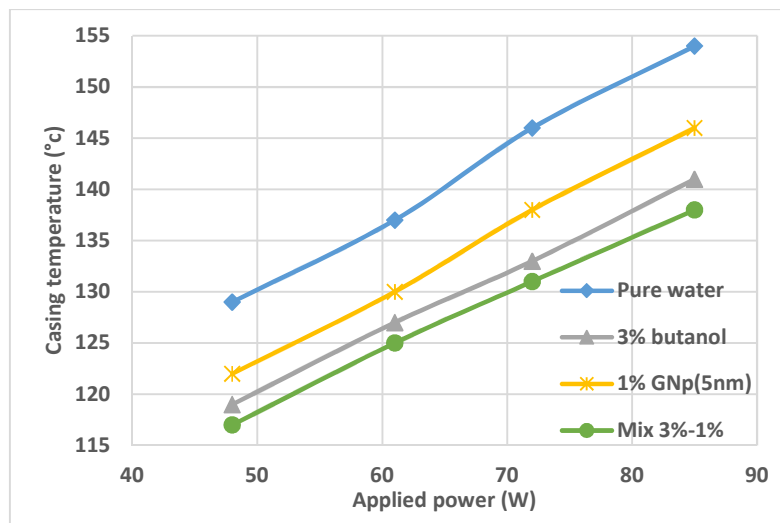

Figure 5. Temporal evolution of the casing temperature for water, self-rewetting fluid (butanol) and gold nanofluid

After measuring the casing temperature and the temperature at the wick inlet, the variation in the thermal resistance as a function of the applied power for the working fluids is shown in **Fig. 5**. It can be seen that the use of a self-rewetting or nanofluids reduce the thermal resistance of evaporator. Also, a mixed solution of butanol self-rewetting gold nanofluid showed the lowest thermal resistance of 22% compared to that of pure water.
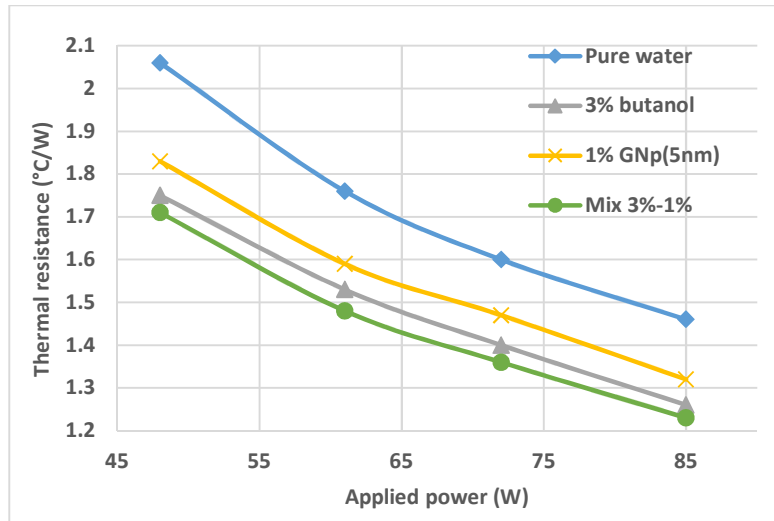

Figure 6. Thermal resistance for water, butanol self-rewetting and gold nanofluids

3.2. Vapor pocket dynamics

In order to understand the enhancement in the thermal performances of the evaporator using nanofluids and self-rewetting solution, the liquid/vapor phase change has been visualized. **Fig. 6**, presents the evolution of the vapor pocket as a function of the applied power for all working fluids. It can be seen that the size of the vapor pocket increases as the applied power increased. This results can be explained by the fact that the increase in the heat load causes a higher vapor mass flow rate at the outlet of the evaporator. As a results, the mass flow rate of the liquid at the outlet of the reservoir also increases, resulting in a lower liquid temperature at the inlet of the wick. Both of these effects tend to stabilize the vapor pocket within the capillary structure. This explanation is in agreement with the numerical results of Boubaker [37] and Ren [38]. So, as the vapor pocket developing inside the porous wick, means a high thermal resistance which promotes overheating of the evaporator casing and affects the thermal performance of the evaporator.
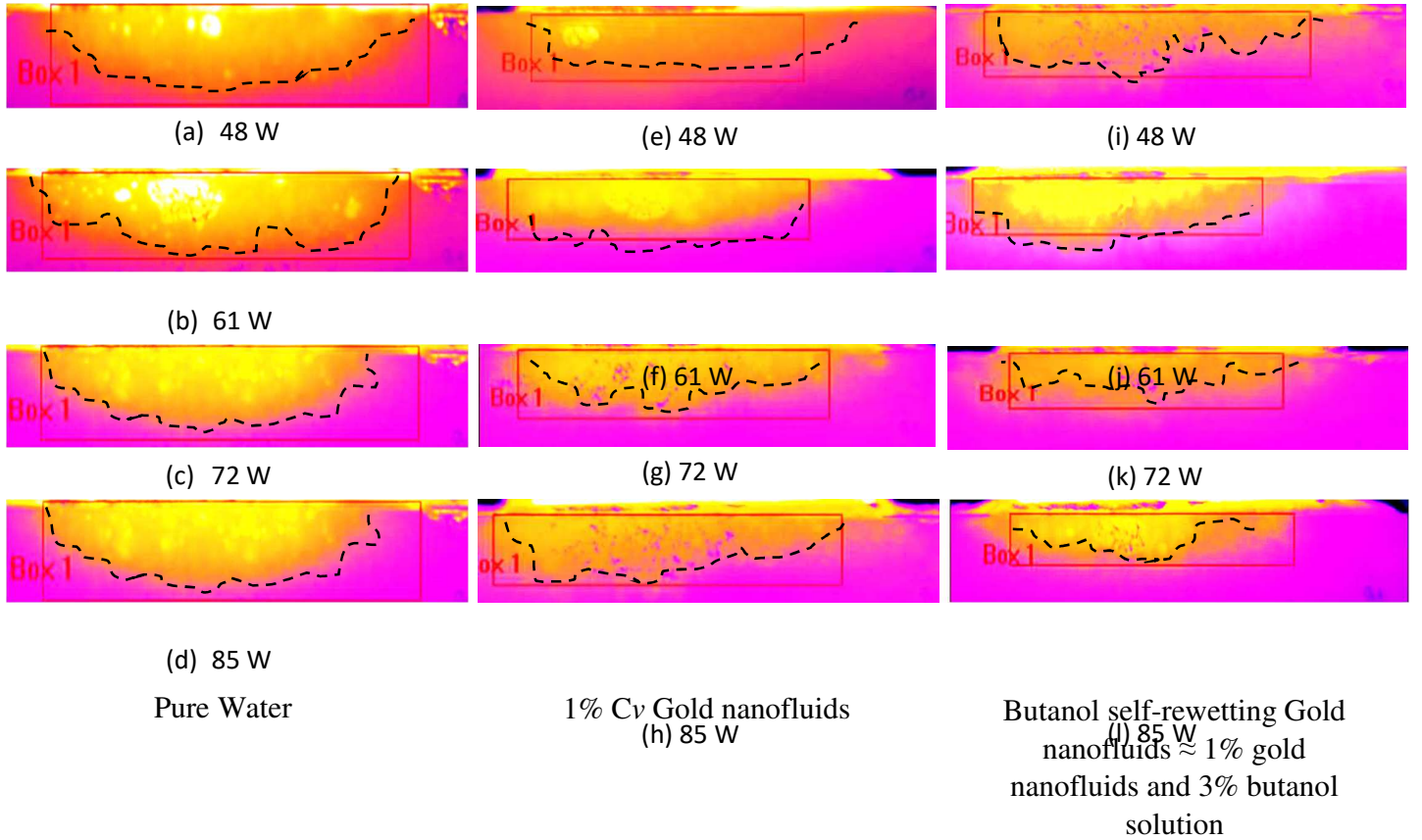
Figure 2. Comparison of the vapor pocket for water, gold nanofluid and self-rewetting nanofluid

For that reason and unlike the water, the vapor zone at the liquid/vapor decrease by increasing the applied power for the gold nanofluid, butanol and self-rewetting nanofluid. The thermal resistance of the vapor pocket inside the capillary structure thus decrease, which explains the decrease in the temperature of the casing evaporator and the increase in thermal performance of the evaporator when it is filled with a butanol self-rewetting gold nanofluid.

To demonstrate how these fluids improved the thermal performance of the CHP evaporator, we presented and calculated the physical properties associated with the thermal conductivity, surface tension (Marangoni forces), wettability, stability and capillarity for each fluid.

The improvement in the thermal performance using gold nanofluid comes mainly from the stability and thermal conductivity of gold nanoparticles in addition to its physical phenomena

associated with the Marangoni cells. The thermal conductivity of gold nanofluid, **Table. 2**, was calculated after applying the model of Leong et al. [39]. It showed the increase in thermal conductivity compared to pure water. Also, the stability of 5nm gold nanoparticles was studied, in my latest work (Zaaroura et al) [40, 41], and showed a good stability inside fluid during droplet evaporation. Moreover, the Marangoni lifetime of same type of nanofluid showed the longest period compared to pure water.

Temperature °C	Thermal conductivity (W/k.m)	
	Water	5 nm, 1% C_v Gold nanofluid
20	0.589	0.662
50	0.651	0.721
90	0.677	0.738

Table 3. Thermal conductivity of gold nanofluid at different temperatures

Whereas, for butanol/water binary mixture, the measured surface tension exceed that of water when the temperature exceeds 99 ° C. From this temperature capillary pumping is more important for butanol aqueous solution (3% C_v). This explain the decrease in the size of the vapor pocket as a function of the applied heat load.

The Marangoni effect takes place when there is a surface tension gradient which can be the results of the existence of a temperature and/or a concentration gradients. As shown in **Fig. 8**, the surface tension, measured using KRUSS pendant method, for butanol solution has a positive gradient form 50 ° C and in this case, the reserve Marangoni flow driven liquid from cold to hot region and as results a decrease in the vapor pocket developed inside the porous section and the casing temperature is significantly reduced.
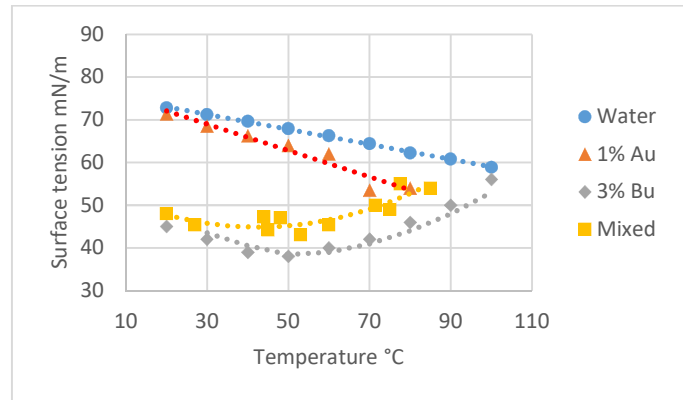
Figure 8. Surface tension measurements for water, butanol (3% C_v), gold (1% C_v), and a mixture of butanol self-rewetting gold nanofluid (Bu 3%-Au 1% C_v) using KRUSS Pendant method, **Appendix B.**

The wettability measurements indicates that adding alcohols, particularly butanol, decrease the contact angle and increase the contact area with metals whatever the nature of the substrate: smooth or porous substrate. It was difficult to measure the contact angle of the water/butanol mixture for porous copper oxide because of its easily and quickly spreading.

Fluids	T_{sur}= 25 °C		T_{sur}= 65 °C	
	Smooth copper	Porous copper	Smooth copper	Porous copper
Water	79.4	70.66	77	73
Gold, 1%C_v	78.3	65	75.6	<30
Butanol, 3% C_v	64	<20	56	Spontaneous spreading
Mixed solution (1%Au/3%Bu/water)	58.1	<10	60	Spontaneous spreading

Table 4. Contact angle measurements, using Drop Shape Analyzer DSA 30s, **Appendix B**

Finally, interesting results were found after a combination of the properties of the self-rewetting butanol solution and gold nanoparticles in a solution in the form of butanol self-rewetting gold nanofluid. This mixture gave the best performance by reducing the thermal resistance of the evaporator by 22 %. It can be seen that the surface tension of this mixture, see **Fig. 8**, increases

with respect to the butanol solution and gives the same behavior. Furthermore, its wettability was improved and maintained spreading above porous substrate.

This mixed gave the best performance by decreasing the evaporator thermal resistance by 22 %. We can find that the surface tension of this mixture increased compared to the butanol solution and provide the same profile.

4. Conclusion

In the current study, the effect of the use of gold nanofluid and self-rewetting fluid (butanol) was investigated experimentally to observe their impact on the heat and mass transfer, inside a porous media, of a two-phase heat transfer device. Several specifications of nanofluids are influential in heat transfer behavior like stability, concentration and the type of nanoparticles. It is found that gold nanofluid (5 nm with 1% C_v) exhibits a very good characteristics in thermal behavior of CHP by reducing system's thermal resistance by 13 % compared to pure water. This enhancement due to the increase in thermal conductivity, Marangoni cells as well as stability of gold nanoparticles indie base fluid. Whereas, the self-rewetting fluid (3% C_v butanol) observed better thermal performance of heat transfer by a 16% reduction in thermal resistance. Due to the positive results, we tested the effect of these two fluids in one solution (1% Au, 3% butanol /water) to combine the properties of gold nanoparticles (thermal conductivity, stability and Marangoni cells) and butanol solution (wettability, Marangoni and capillary forces). The 22% lower thermal resistance is finally observed and the best performance is obtained in the CHP. All these thermophysical properties were responsible for decreasing the vapor pocket area compared to the base fluid.

Author Information
Corresponding Author

*Email: souad.harmand@uphf.fr

    Ibrahim.zaaroura@hotmail.com

Appendix A. Technical FLIR specification

See Fig. 9.

| System Overview	SC7210-7500 / SC7300
Waveband	MW
Sensor type	InSb / MCT
Pixel Resolution	320x256
Pixel Pitch	30μm
Spectral ranges	1.5 - 5.1 μm for InSb (BB)
Measurement	
NETD	<20mK for InSb
Standard Camera Calibration Range	5ºC to 300ºC for InSb
Optional Camera Calibration Range	-20°C to 300ºC
Digital Full Frame rate	InSb: 190 Hz - 380 Hz full frame up to 3 kHz - 39.8 kHz with windowing

Figure 9. Technical FLIR specification

Appendix B. Drop Shape Analyzer

Measurement specifications	DSA30B	DSA30S	DSA30E
Sessile drop/Captive bubble			
Result		contact angle	
Range [4]		0 to 180°	
Resolution [4]		0.01°	
Accuracy [5]		0.1°	
Models		conic section, polynom, circle, Young-Laplace, height-width	
Types [6]		advancing, receding, static, dynamic, tilting	
Surface free energy of solids [2]			
Result		surface free energy	
Models	equation of states, Zisman, Fowkes, Wu, Owens-Wendt-Rabel-Kaelble, Schultz-1, Schultz-2, extended Fowkes, acid-base theory		
Pendant drop/Rising drop [2, 3]			
Results		interfacial and surface tension	
Range [4]		0.01 to 2000 mN/m	
Resolution [4]		0.01 mN/m	
Model		Young-Laplace	
Types		static, dynamic	

Figure 10. Drop shape Analyzer technical properties, KRUSS System DSA30S

The surface tension measurements were done using DSA 30s KRUSS system with pendant drop method. The pendant droplet was formed in a closed control air chamber environment (Air/liquid) as presented in **Fig. 12**. The temperature of the chamber (From ambient to 95 °C) was controlled by the heater and thermostat which were connected to the KRUSS system.
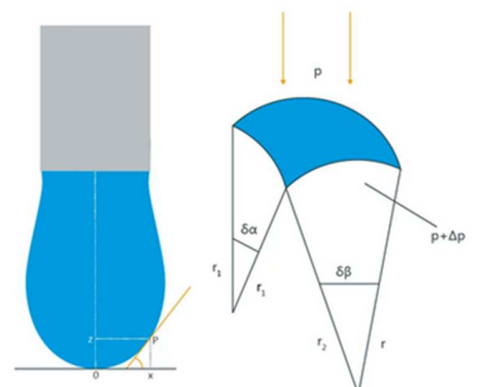
For pendant drop method, measuring the surface tension is described by the Young-Laplace equation:

$$\Delta_p = \sigma . \left(\frac{1}{r_1} + \frac{1}{r_2} \right)$$

Where, is the pressure difference, r_1 and r_2 are the radii of curvature of the surface, **Fig. 11**.
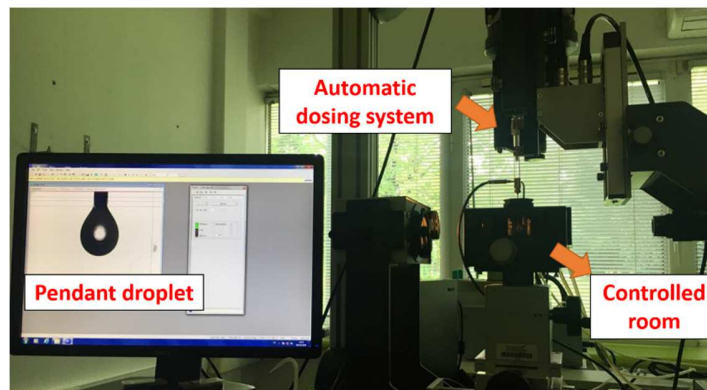
Figure 11. Pendant drop

Figure 12. Drop Shape Analyzer DSA 30s, KRUSS system, LAMIH Laboratory, France

The same KRUSS system instrument, in sessile droplet mode, was used for wettability measurements on the smooth and porous copper medium. For these measurements, we used same initial droplet volume, under same conditions (V_i=1.5 ul, heated surface (T_{sur}=25°C and T_{sur}=60°C) and chamber temperature =25 °C), deposited on the surface to measure and compare the contact angle for each fluids.
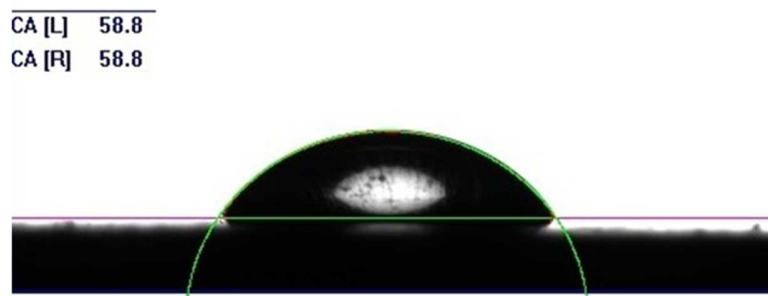

Figure 13. Contact angle measurement for the mixed solution droplet (1%Au/3%Bu/water) on a smooth copper surface at ambient temperature, T_{sur}=25°C.

References

[1] Y. huibin, G. Xuenong, D. Jing, Z. Zhengguo, F. Yutang, Thermal management of electronic components with thermal adaptation composite material, Applied Energy 87 (2010) 3784-3791.

[2] X. Ji, J. Xu, H. Li, G. Huang, Switchable heat transfer mechanisms of nucleation and convection by wettability match of evaporator and condenser for heat pipes: Nano-structured surface effect, Nano Energy, 38 (2017), 313-325.

[3] S. Xu, Y. Tu, P. Huang, C. Luan, Z. Wang, B. Shi, H. Liu, Z. Liu, Effects of wall temperature on methane MILD combustion and heat transfer behaviors with non-preheated air, Appl. Therm. Eng, 174 (2020), 115282.

[4] B. Zhao, K. Chen, S. Buddhiraju, G. Bhatt, M. Lipson, S. Fan, High-performance near-field thermophotovoltaices for waste heat recovery, Nano Energy, 41 (2017), 344-350.

[5] H. Tang, Y. Tang, Z. Wan, J. Li, W. Yuan, L. Lu, Y. Li, K. Tang, Review of applications and developments of ultra-thin micro heat pipes for electronic cooling, Applied Energy 223 (2018) 383-400.

[6] V. Singh, D. Haridas, A. Srivastava, Experimental study of heat transfer performance of compact wavy channel with nanofluids as the coolant medium: Real time non-intrusive measurements, Int. J. Therm. Sci, 145 (2019) 105993.

[7] P. Kanti, K. V. Sharma, C. G. Ramachandra, M. Gupta, Thermal performance of fly ash nanofluids at varous inlet fluid temperatures : An experimental study, International communications in Heat and Mass Transfer, 119 (2020) 104926.

[8] Y. Jiang, X. Zhou, Y. Wang, Effect of nanoparticles shapes on nanofluid mixed forced and thermocapillary convection in minichannel, International communications in Heat and Mass Transfer, 118 (2020) 104884.

[9] A. M. Hussein, Thermal performance and thermal properties of hybrid nanofluid laminar flow in a double pipe heat exchanger, Exp. Thermal Fluid Sci, 88 (2017) 37-45.

[10] E. Cuce, T. Guclu, P. M. Cuce, Improving thermal performance of thermoelectric coolers (TECs) through a nanofluid driven water to air heat exchanger design: An experimental research, Energy Convers Manage, 214 (2020) 112893.

[11] I. Nurdin, I. I. Yaacob, M. R. Johan, Enhancement of thermal conductivity and kinematic viscosity in magnetically controllable, maghemite (γ –Fe_2O_3) nanofluids, Exp. Thermal Fluid Sci, 77 (2016) 265-271.

[12] M. Karimzadehkhouei, M. Shojaeian, K. Sendur, M.P. Menguc, A. Kosar, The effect of nanoparticles type and nanoparticle mass fraction on heat transfer enhancement in pool boiling, Int. J. Heat Mass Transfer 109 (2017) 157-166.

[13] R. Agarwal, K. Verma, N. K. Agrawal, R. Singh, Sensitivity of thermal conductivity for Al_2O_3 nanofluids. Exp. Thermal Fluid Sci, 80 (2017) 19-26.

[14] A. Nasiri, M. S. Niasar, A. Rashidi, A. Amrollahi, R. Khodafarin, Effect of dispersion method on thermal conductivity and stability of nanofluid, Exp. Thermal Fluid Sci, 35 (2011) 717-723.

[15] J. P. Vallejo, E. Sani, G. Zyla, L. Lugo, Tailored silver/graphene nanoplatelet hybrid nanofluids for solar applications, J. Mol. Liq, 296 (2019) 112007.

[16] G. Huminic A. Huminic, Heat transfer capability of the hybrid nanofluids for heat transfer applications, J. Mol. Liq 272 (2018) 857-870.

[17] B.A. Suleimanov, F.S. Ismailov, E.F. Veliyev, Nanofluid for enhanced oil recovery, J. Petrol. Sci. Eng, 78 (2011) 431-437.

[18] Z. H. Liu, Y. Y. Li, R. Bao, Thermal performance of inclined grooved heat pipes using nanofluids, Int. J. Therm. Sci, 49 (2010) 1680-1687.

[19] H. Maddah, M. Ghazvini, M. H. Ahmadi, Predicting the efficiency of CuO/water nanofluid in heat pipe heat exchanger using neural network, 104 (2019) 33-40.

[20] E. Khajehpour, A. R. Noghrehabadi, A. E. Nasab, S. M. Hossein, Experimental investigation of the effect of nanofluids on thermal resistance of a thermosiphon L-shape heat pipe at different angles, International communications in Heat and Mass Transfer 113 (2020) 104549.

[21] J. P. Vallejo, U. Calvino, I. Freire, J. F. Seara, L. Lugo, Convection heat transfer in pipe flow for glycolated water-based carbon nanofluids. A thorough analysis, J. Mol. Liq 301 (2020) 112370.

[22] M. Singh, Capillarity enhancement of micro heat pipes using grooves with variable apex angle, Int. J. Therm. Sci, 150 (2020) 106239.

[23] Y. Maydanik, Loop heat pipes, Appl. Therm. Eng 25 (5) (2005) 635-657.

[24] M.O. Hamdan, Loop Heat Pipe (LHP) Modeling and Development by Utilizing Coherent Porous Silicon (CPS) Wicks, PhD thesis, University of Cincinnati, 2003.

[25] Cecere, A., Di Martino, G.D., Mungiguerra, S. Experimental Investigation of Capillary-Driven Two-Phase Flow in Water/Butanol under Reduced Gravity Conditions, Microgravity Science and Technology, August 2019, Volume 31, Issue 4, pp 425-434.

[26] R. Savino, R. Di Paola, A. Cecere, R. Fortezza, Self-rewetting heat transfer fluids and nanobrines for space heat pipes, Acta Astronautica 67 (2010) 1030-1037.

[27] A. Cecere, R. D. Paola, R. Savino , Y. Abe, L. Carotenuto, S.V. Vaerenbergh, Observation of Marangoni flow in ordinary and self-rewetting fluids using optical diagnostic systems, Eur. Phys. J. Special Topics 192, 109-120 (2011).

[28] R. Savino, D. De Cristofaro, A. Cecere, Flow visualization and analysis of self-rewetting fluids in a model heat pipe, International Journal of Heat and Mass Transfer 115 (2017) 581-591.

[29] R. Savino, N. di Francescantonio, R. Fortezza, Y. Abe, Heat pipes with binary mixtures and inverse marangoni effects for microgravity applications, Acta Astronautica 61 (1) (2007) 16-26.

[30] R. Savino, A. Cecere, R. Di Paola, Surface tension-driven flow in wickless heat pipes with self-rewetting fluids, International Journal of Heat and Fluid Flow, International Journal of Heat and Fluid Flow 30 (2009) 380-388.

[31] T. P. Teng, H. G. Hsu, H. E. Mo, C. C. Chen, Thermal efficiency of heat pipe with alumina nanofluid, J. Alloy. Compd., 504 (2010) S380-S354.

[32] S.W. Kang, W.C. Wei, S.H. Tsai, S.Y. Yang, Experimental investigation of silver nano-fluid on heat pipe thermal performance, Appl. Therm. Eng, 26 (2006) 2377-2382.

[33] I. Zaaroura, S.Harmand, J. Carlier, R. Boukherroub, Evaporation of Gold Nanofluid Sessile drops on heated substrate, TechConnect Briefs, (2019) 37-41.

[34] R. Boubaker, S. Harmand, S. Ouenzerfi, Effect of self-rewetting fluids on the liquid/vapor phase change in a porous media of two-phase heat transfer devices, Int. J. Heat Mass Transfer, 136 (2019) 655-663.

[35] R. J. Moffat, Describing the uncertainties in experimental results, Experimental Thermal and
Fluid Science 1 (1) (1988) 3-17.

[36] R. Boubaker, S. Harmand, V. Platel, Experimental study of the liquid/vapor phase change in a porous media of two-phase heat transfer devices, Appl. Therm. Eng, 143 (2018) 275-282.

[37] R. Boubaker, V. Platel, Vapor pocket behavior inside the porous wick of a capillary pumped Loop for terrestrial application, Applied Thermal Engineering 84 (2015) 420-428.

[38] C. Ren, Q.S. Wu, M.B. Hu, Heat transfer with flow and evaporation in loop heat pipes wick at low or moderate heat fluxes, Int. J. Heat Mass Transfer 50 (11) (2007) 2296-2308.

[39] K.C. Leong, C. Yang, S.M.S. Murshed, A model for the thermal conductivity of nanofluids-the effect of interfacial layer, J. Nanoparticle Res., 8 (2) (2006), pp. 245-254.

[40] I. Zaaroura, M. Toubal, H. Reda, J. Carlier, S. Harmand, R. Boukherroub, A. Fasquelle, B. Nongaillard "Evaporation of nanofluid sessile drops: Infrared and acoustic methods to track the dynamic deposition of copper oxide nanoparticles", Int. J. Heat Mass Transfer 127, Part B (2018) 1168-1177.

[41] I. Zaaroura, S. Harmand, J. Carlier, M. Toubal, A. Fasquelle, B. Nongaillard, Experimental studies on evaporation kinetics of gold nanofluid droplets: Influence of nanoparticle sizes and coating on thermal performance, Appl. Therm. Eng., 183 (2021) 116180.